Comparison of different GMT-based approaches to calculate the field distribution in rectangular cavities

J. Fröhlich, G. Klaus
Swiss Federal Institute of Technology
CH-8092 Zurich

ABSTRACT

Different GMT based approaches are applied to the problem of field distributions inside shielded rooms. These approaches are discussed and compared by means of modelling, computation time and accuracy of the results compared to a reference solution. The aim is to find a calculation procedure which allows one to compute the frequency behaviour of different test setups and different environment parameters. The usual MMP approach with a special placement of the expansion functions turns out to be the most efficient and accurate way to solve this kind of problem.

1. INTRODUCTION

The knowledge of field distributions in cavities with conductive walls is of increasing interest for EMC applications and communication inside buildings. For the simulation of different test setups over a wide frequency range an efficient calculation procedure is necessary because it is not very efficient to model and optimise the whole setup for every single frequency. For this purpose three different GMT - based approaches are compared.

The GMT (Generalised Multipole Technique) [1] is a method for numerically solving static and time-harmonic electromagnetic boundary and eigenvalue problems within piecewise linear and homogeneous domains. An expansion for the unknown field is made with analytic solutions of the Helmholtz equations in cylindrical and spherical coordinates. Other solutions of Maxwell's equations, which can be more efficient for special geometries, can easily be included.

The approximate numerical solution of the boundary value problem is a linear combination of basis functions. A linear system of equations for the coefficients in the expansion can be obtained by minimising the remaining mismatching error on the boundary with various methods.

2. MATHEMATICAL PROBLEM FORMULATION

Considering time-harmonic electromagnetic fields in piecewise linear, homogeneous and isotropic domains, leads to the following problem formulation:

$$\mathrm{rot}\underline{\vec{E}}(\vec{r}) - i\omega\mu(\vec{r})\underline{\vec{H}}(\vec{r}) = 0 \qquad (1)$$

$$\mathrm{rot}\underline{\vec{H}}(\vec{r}) + i\omega\varepsilon'(\vec{r})\underline{\vec{E}}(\vec{r}) = \underline{\vec{J}}_0(\vec{r}) \qquad (2)$$

where $\varepsilon'(\vec{r}) = \varepsilon(\vec{r}) + i\sigma(\vec{r})/\omega$ is the complex dielectric constant and $\underline{\vec{J}}_0(\vec{r})$ denotes the impressed current distribution.

Out of the first equation it follows:

$$\mathrm{div}(\mu(\vec{r})\underline{\vec{H}}(\vec{r})) = 0 \qquad (3)$$

$$\mathrm{div}(\varepsilon'(\vec{r})\underline{\vec{E}}(\vec{r})) = -(i/\omega)\mathrm{div}\underline{\vec{J}}_0(\vec{r}) \qquad (4)$$

Because of the linearity of equations (1), (2), (3) and (4) the fields can be split into a source-free part and a part containing the source. With

$$\underline{\vec{E}}(\vec{r}) = \underline{\vec{E}}^F(\vec{r}) + \underline{\vec{E}}^S(\vec{r}) \qquad (5)$$

$$\underline{\vec{H}}(\vec{r}) = \underline{\vec{H}}^F(\vec{r}) + \underline{\vec{H}}^S(\vec{r}) \qquad (6)$$

we have

$$\mathrm{rot}\underline{\vec{E}}^S(\vec{r}) - i\omega\mu(\vec{r})\underline{\vec{H}}^S(\vec{r}) = 0 \qquad (7)$$

$$\mathrm{rot}\underline{\vec{H}}^S(\vec{r}) + i\omega\varepsilon'(\vec{r})\underline{\vec{E}}^S(\vec{r}) = \underline{\vec{J}}_0(\vec{r}) \qquad (8)$$

and

$$\mathrm{rot}\underline{\vec{E}}^F(\vec{r}) - i\omega\mu(\vec{r})\underline{\vec{H}}^F(\vec{r}) = 0 \qquad (9)$$

$$\mathrm{rot}\underline{\vec{H}}^F(\vec{r}) + i\omega\varepsilon'(\vec{r})\underline{\vec{E}}^F(\vec{r}) = 0 \qquad (10)$$

Now assuming that the whole space can be split into K domains $D_k, k = 1..K$ each having linear, homogenous and isotropic material properties, plus one not necessarily connected fieldfree domain D_0,

the material properties can be written as $\varepsilon(\vec{r}) = \varepsilon_k$, $\mu(\vec{r}) = \mu_k$ and $\sigma(\vec{r}) = \sigma_k$ for $\vec{r} \in D_k, k = 1..K$. In each domain the field is split according to (9) and (10) and the part containing the source is given in terms of the field values in the domain D_k satisfying the equations (7) and (8). The determination of these field values out of a given $\underline{\vec{J}}_0(\vec{r})$ is a separate problem which can be used to include different excitations.

This leads to the final formulation : The electromagnetic field in piecewise homogeneous, linear and isotropic three dimensional space for the source free part $\underline{\vec{E}}_k^F(\vec{r}), \underline{\vec{H}}_k^F(\vec{r})$ can be determined by applying the equations :

$$\mathrm{rot}\,\underline{\vec{E}}_k^F(\vec{r}) - i\omega\mu_k \underline{\vec{H}}_k^F(\vec{r}) = 0 \qquad (11)$$

$$\mathrm{rot}\,\underline{\vec{H}}_k^F(\vec{r}) + i\omega\varepsilon'_k \underline{\vec{E}}_k^F(\vec{r}) = 0 \qquad (12)$$

for $\vec{r} \in D_k, k = 1...K$

with boundary conditions :

$$\vec{n}(\vec{r}) \times \left(\underline{\vec{E}}_i^F(\vec{r}) - \underline{\vec{E}}_k^F(\vec{r})\right) = \vec{n}(\vec{r}) \times \left(\underline{\vec{E}}_i^S(\vec{r}) - \underline{\vec{E}}_k^S(\vec{r})\right)$$

$$\vec{n}(\vec{r}) \times \left(\underline{\vec{H}}_i^F(\vec{r}) - \underline{\vec{H}}_k^F(\vec{r})\right) = \vec{n}(\vec{r}) \times \left(\underline{\vec{H}}_i^S(\vec{r}) - \underline{\vec{H}}_k^S(\vec{r})\right)$$

$$\vec{n}(\vec{r}) \times \left(\underline{\vec{H}}_i^F(\vec{r}) - \underline{\vec{H}}_k^F(\vec{r})\right) = \vec{n}(\vec{r}) \times \left(\underline{\vec{H}}_i^S(\vec{r}) - \underline{\vec{H}}_k^S(\vec{r})\right)$$

$$\vec{n}(\vec{r}) \cdot \left(\varepsilon'_i \underline{\vec{E}}_i^F(\vec{r}) - \varepsilon'_k \underline{\vec{E}}_k^F(\vec{r})\right) = \vec{n}(\vec{r}) \cdot \left(\varepsilon'_i \underline{\vec{E}}_i^S(\vec{r}) - \varepsilon'_k \underline{\vec{E}}_k^S(\vec{r})\right)$$

$$\vec{n}(\vec{r}) \cdot \left(\mu_i \underline{\vec{H}}_i^F(\vec{r}) - \mu_k \underline{\vec{H}}_k^F(\vec{r})\right) = \vec{n}(\vec{r}) \cdot \left(\mu_i \underline{\vec{H}}_i^S(\vec{r}) - \mu_k \underline{\vec{H}}_k^S(\vec{r})\right)$$

$$\text{for } \vec{r} \in \partial D_{ik}, ik > 0, i \neq k \qquad (13)$$

or for the boundary to the domain D_0 :

$$\vec{n}(\vec{r}) \times \underline{\vec{E}}_i^F(\vec{r}) = \vec{n}(\vec{r}) \times \underline{\vec{E}}_i^S(\vec{r}),$$

$$\vec{n}(\vec{r}) \cdot \mu_i \underline{\vec{H}}_i^F(\vec{r}) = \vec{n}(\vec{r}) \cdot \mu_i \underline{\vec{H}}_i^S(\vec{r}),$$

$$\text{for } \vec{r} \in \partial D_{i0}, i \neq 0 \qquad (14)$$

3. MULTIPLE MULTIPOLE CODE (MMP)

The MMP code [2,3] is an implementation of the formulation given above. The field $\underline{\vec{f}}_i(\vec{r})$ in each domain i is expanded as a linear combination of basis functions $\underline{\vec{f}}_{ij}(\vec{r})$

$$\underline{\vec{f}}_i(\vec{r}) = \sum_{j=1}^{n} \underline{c}_{ij} \underline{\vec{f}}_{ij}(\vec{r}), \qquad (15)$$

where the $\underline{\vec{f}}_{ij}(\vec{r})$ are analytical solutions of the time-harmonic Maxwell equations.

The coefficients $\underline{c}_{ij}$ are obtained by enforcing the boundary conditions for all field components in discrete matching points on the boundary. Using the *"Generalized Point Matching Technique"* with more matching points than necessary (factor 3-10) leads to an over determined system of equations

$$A \cdot c = b, \qquad (16)$$

where A is a rectangular m by n matrix, c the parameter vector and b the inhomogeneity resulting from the excitation.

Because more than one basis function is taken for one single domain, numerical dependency has to be avoided. There are some geometrical rules which have to be fulfilled. These are also implemented in an *"Automatic Pole Setting Routine"* [4].

The MMP solution is taken as a reference for comparing the results of the other methods which are not validated as often. So these solutions are not optimised according to discretisation, expansion setting and computation time. The aim of these (MMP) computations was to have very accurate solutions according to the boundary conditions.

4. THE SURFACE IMPEDANCE BOUNDARY CONDITIONS (SIBC) IN THE MMP CODE

The surfaces of domains with a high refractive index can be modelled with *"surface impedance boundary conditions"*. The field within the refractive domain D_j is approximated by vertically entering plane waves - explicit expansions for the field within the domain are not made.
In the coordinate system of the matching point the equations are:

$$\underline{E}_{t1}^i = -\underline{Z}_j \cdot \underline{H}_{t2}^i \qquad (17)$$

$$\underline{E}_{t2}^i = \underline{Z}_j \cdot \underline{H}_{t1}^i, \qquad (18)$$

$$\text{with } \underline{Z}_j = \sqrt{\frac{\mu}{\varepsilon'}}; \quad \varepsilon' = \varepsilon + j\frac{\sigma}{\omega}.$$

The mismatching error is taken as

$$\mathrm{sperr}^2 = \rho_k^2 = \frac{1}{2}\left[\left|\underline{\vec{E}}_{t1}^i + \underline{Z}_j \cdot \underline{\vec{H}}_{t2}^i\right|^2 + \left|\underline{\vec{E}}_{t2}^i - \underline{Z}_j \cdot \underline{\vec{H}}_{t1}^i\right|^2\right] \qquad (19)$$

For high conductivities the surface impedance boundary condition turns into the boundary condition for perfect conductors.

5. CONDUCTIVE WALLS

For problems with conductive walls one has to deal with reflections. As a solution a modified *"image charge principle"* for dynamics seems to be obvious. The basic idea of this approach is to place appropriate image sources on the points of reflection and to orient them according to the rules of reflection. This is valid for ideal conducting planes and walls, where the image sources are exactly the same as the exciting source. For lossy materials, the physical behaviour of the image sources is no longer exactly the same. For a multipole source over conducting ground, a *"numerical exact image"* can be determined, consisting of the multipole source and some higher order multipole terms. These higher order terms have more and more influence as the conductivity decreases. By increasing the conductivity towards infinity these higher order terms will disappear. This has been demonstrated using the MMP code for the calculation of a dipole over conductive ground (Fig. 1 and 2).

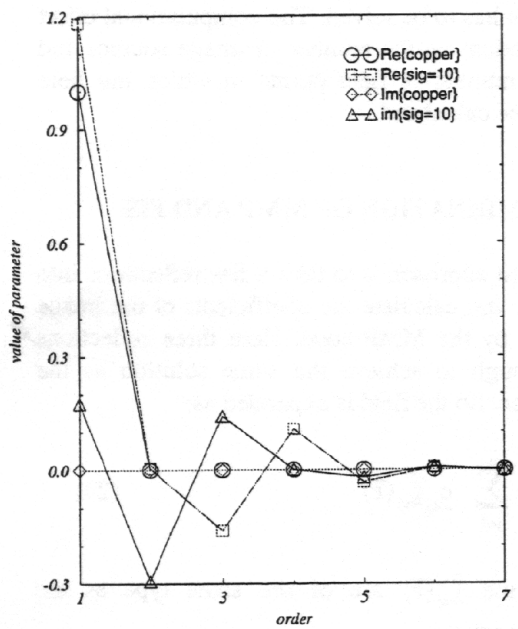

Figure 1: Values of real and imaginary parts of the parameters of the multipole orders 1 to 7 fo/r conducting ground with conductivity 5.6e7(copper) and 10 (~seawater) which is about the range of the SIBC.

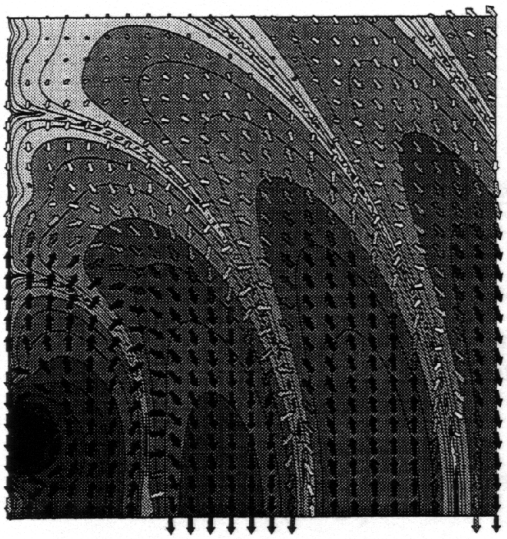

Figure 2: Example of a field distribution (iso-lines: absolute value of Poynting vector and arrows: E-field) of a vertical dipole over conducting ground (σ=10).

6. DEALING WITH MULTIPLE REFLECTIONS

The easiest problem with multiple reflections is that of a source between two interfaces. Here a dipole is taken between two ideal conducting interfaces. With this example the principle of the other two approaches will be shown.

The MMP solution of this problem is to place two higher order multipoles on the first points of reflection. This is taken as a reference.

Due to the parallel walls the source is mirrored on both interfaces and every mirrored source is mirrored again. This leads to an infinite number of images which represent the reflections and the re-reflections of the original. Because the influence of the image sources decreases with distance, only a finite number of image sources has to be taken into account. This way of calculating the field is implemented as *"Finite Image Source Method"*.

7. FINITE IMAGE SOURCE METHOD (FIS)

Starting with a rectangular cavity the field is expanded as an array of image sources. The Field components can be represented by:

$$\underline{F}(\vec{r}) = \sum_{i=-\infty}^{\infty} \sum_{j=-\infty}^{\infty} \sum_{k=-\infty}^{\infty} \underline{R}_{ijk} \underline{F}_{ijk}(\vec{r}) \quad (20)$$

where

$$\underline{R}_{ijk} = \underline{R}^{lx_+}_{x_+} \cdot \underline{R}^{lx_-}_{x_-} \cdot \underline{R}^{ly_+}_{y_+} \cdot \underline{R}^{ly_-}_{y_-} \cdot \underline{R}^{lz_+}_{z_+} \cdot \underline{R}^{lz_-}_{z_-} \qquad (21)$$

$\underline{R}^{lp_{+\alpha-}}_{p_{+\alpha-}}$ is the reflection factor of the corresponding wall after l reflections (p stands for x,y,z). It is calculated as

$$\underline{R}^{lp_{+\alpha-}}_{p_{+\alpha-}} = \underline{R}_p(\sigma,\omega)^l = \left(\frac{\underline{k}_c - \underline{k}_p}{\underline{k}_c + \underline{k}_p}\right)^l \qquad (22)$$

where the index 'p' stands for the domain of the corresponding wall and 'c' for the inner domain (the inside of the cavity).

The number of additional image sources on the l^{th} layer taken into account is:

$$N_l = 4l^2 + 2. \qquad (23)$$

For the case of the two ideal conducting interfaces the reflection coefficient of the two interfaces is taken as one and the other reflection coefficients are left zero. Looking at the convergence behaviour towards the reference solution one can see that the influence of the image sources decreases rapidly and a finite number of image sources is enough to achieve a stable solution. The average difference between the FIS solution and the one obtained with MMP is 2.5e-4[V/m] or 1.6 %. (Fig. 3 and 4)

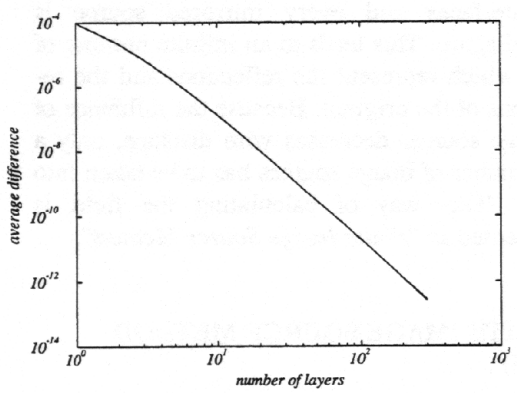

Figure 3: Average difference of 500 field points of the solution with n layers and the solution with n-1 layers versus the number of layers n for a dipole between two interfaces.

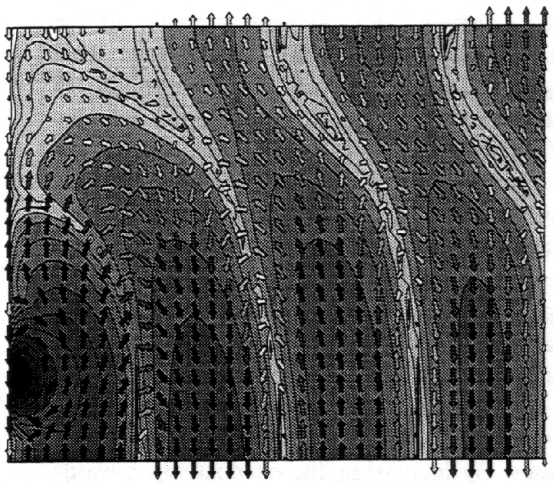

Figure 4: Example of the field distribution of a vertical dipole between two ideally conducting interfaces.

The advantage of this approach is that no system of equation has to be solved. The computational effort is dependent on the number of image sources and on the number of field points in which the field should be calculated.

8. COMBINATION OF MMP AND FIS

The third approach is to take a few reflections into account and calculate the coefficients of the image sources by the MMP code. Here three reflections are enough to achieve the same solution as the reference. So the field is expanded as:

$$\vec{\underline{f}}_c(\vec{r}) = \sum_{j=1}^{n} \underline{c}_{cj} \vec{\underline{f}}_{cj}(\vec{r}) \qquad (24)$$

where the $\vec{\underline{f}}_{cj}(\vec{r})$ are of the same type as the exciting source.

The comparison of the results is carried out with the following comparison criteria:

9. COMPARISON CRITERIA

- average of field value:

$$\bar{f} = \frac{1}{N}\sum_{i=1}^{N}\frac{1}{6}\left|\underline{\vec{E}}_i + \underline{Z}_0 \cdot \underline{\vec{H}}_i\right| \qquad (25)$$

- average of field change between the fields f_1 and f_2 or average field difference:

$$\bar{f}_{change} = \frac{1}{N}\sum_{i=1}^{N}\frac{1}{6}\left[\left|\underline{\vec{E}}_{i1} - \underline{\vec{E}}_{i2}\right| + \underline{Z}_0\left|\underline{\vec{H}}_{i1} - \underline{\vec{H}}_{i2}\right|\right] \qquad (26)$$

- the mismatching error on the boundary (not used for FIS)

- visualisation of the field distribution (qualitative criteria)

Now the next step is to look at the behaviour of these three approaches calculating the field distribution inside a lossy rectangular cavity. The MMP solution is taken again as reference, the mismatching error on the boundary is in the range of *0.1%*.

10. LOSSY RECTANGULAR CAVITY CALCULATED WITH FIS AND THE COMBINED APPROACH

In a cavity with finite conductive walls the eigenvalues have a small imaginary part, thus the source-free modes would exist only for complex values of ω, which means that they will never be excited without a source. When the walls are lossy, only source excited solutions are possible and the internal domain problem can be formulated according to the equations (5) to (14). The solution for this kind of problem is unique [6].

The field distribution in a lossy rectangular cavity has been calculated for 30 / 100 / 300 MHz and for σ = 5.6e7 (copper) and 10 (~seawater). In this range for the value of sigma, the *"surface impedance boundary conditions"* can be applied.

First the convergence towards a stable solution is shown and as a further step the convergence towards the reference. The geometry of the cavity is 5m*7m*4m, which means that 30MHz is below the first resonance frequency and 100MHz and 300MHz are near resonant frequencies.

With FIS the field is calculated taking 150 layers into account. The field distribution is calculated on a regular grid of 500 points. For highly conductive walls even with 150 layers the solution is not stable for all frequencies. For σ=10 S/m the solution converges towards a stable solution but only for low frequencies towards the reference.

Using the combined approach one obtains the same solution as the reference for all frequencies but with fewer parameters to be determined. The computation time is dependent on $M \cdot N^2$ where M is the number of matching points and N is the number of parameters to be determined (Fig. 5 and 6).

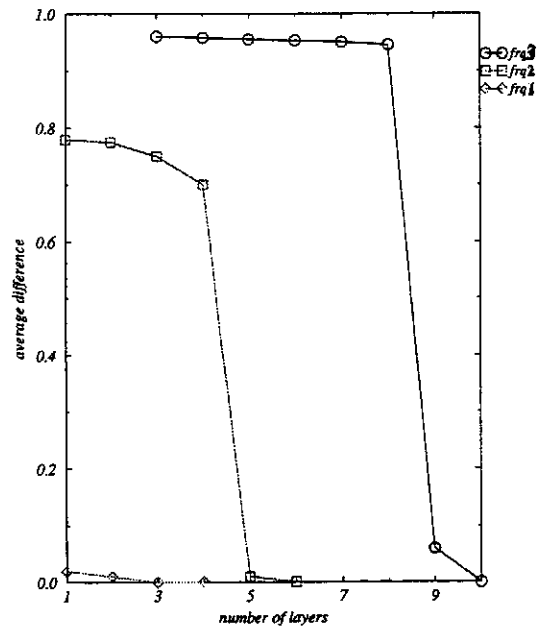

Figure 5: Average difference over 500 field points of the solution of the combined approach and the reference solution versus the number of layers taken into account („wall-conductivity" 5.6e7 S/m, frq1=30MHz, frq2= 100MHz, frq3=300MHz).

11. CONCLUSIONS

The often proposed mirror principle is not efficient for calculating field distributions with many field points and for highly conductive walls. It is useful for finding an optimal expansion setting for the two other methods compared here. Also, it can be used to calculate the field in one point, or the field distributions when only one or two walls are present.

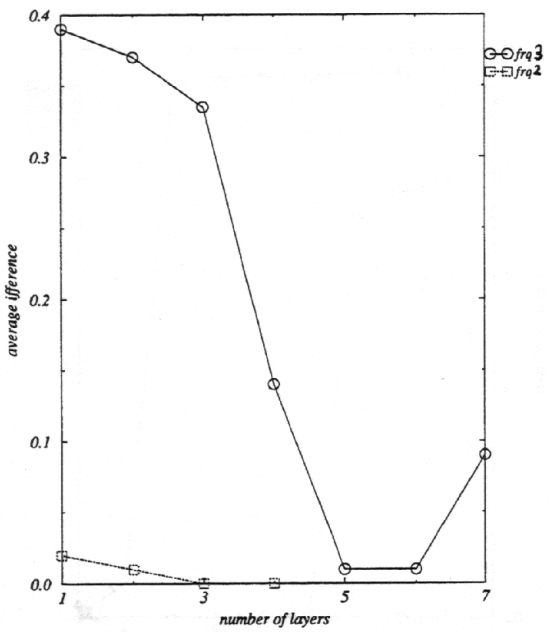

Figure 6: Average difference over 500 field points of the solution of the combined approach and the reference solution versus the number of layers taken into account (conductivity is 10 S/m, frq1=30MHz not visible on the 0.0 line, frq2=100MHz, frq3=300MHz).

The most efficient approach of those compared here, for calculating the field distributions in lossy rectangular cavities, is the combined approach. This approach can be seen as the same as MMP with a very special input configuration and one can carry out calculations of the field behaviour over a wide frequency range with a single model.

12. OUTLOOK

An efficient approach has been found for obtaining accurate solutions according to the boundary conditions. For deeper insight into the accuracy, the solutions have to be validated performing appropriate measurements.

Another step has already been carried out namely the problem of a scatterer placed inside

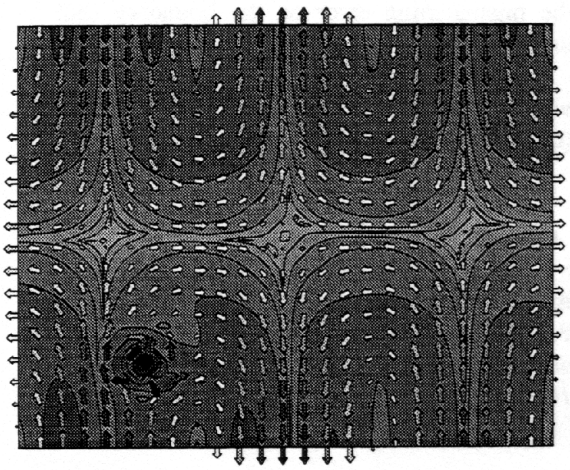

Figure 7: Field distribution in a rectangular cavity of 5m/7m/4m at a frequency of 100MHz.

the cavity. This will be used to study the influences of scattering objects on the standing wave patterns depending on their geometry and their location [8].

Further, the frequency behavior of different setups of rectangular cavities has been calculated, e.g. different location of the source and different materials on the walls [9].

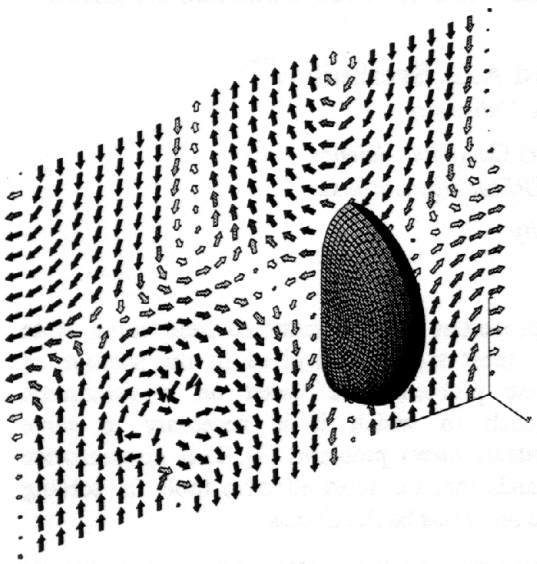

Figure 8: Field distribution of a rectangular cavity with a scatterer inside.

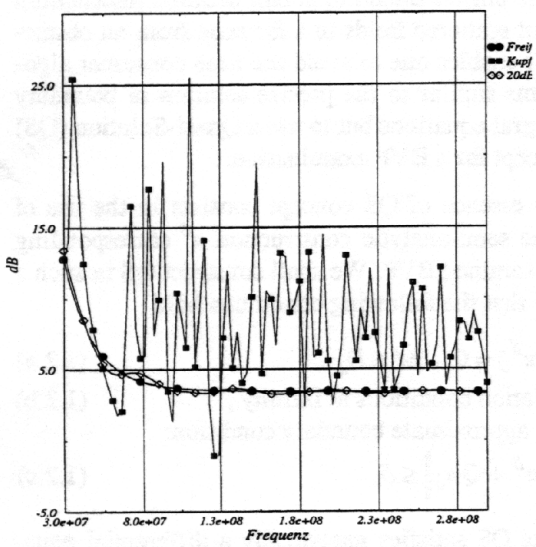

Figure 9: Example of the averaged E-Field value over a region of $1m^3$ placed 1m away from the source versus frequency for different material properties of the walls. Meaning of legends: "Freifeld": Dipole without cavity, "Kupfer": walls of copper, "20dB": walls with 20dB attenuation according to a plane wave with normal incidence on a conducting half space (absorber-lined chamber).

13. REFERENCES

[1] C. Hafner, *"The Generalised Multipole Technique for Computational Electromagnetics"*, Artech House, Inc., Boston, 1990.

[2] L. H. Bomholt, *"MMP-3D - A Computer Code for Electromagnetic Scattering Based on the GMT"*, Diss. ETH No.9225, Zurich, 1990.

[3] G. Klaus, *"3-D Streufeldberechnungen mit Hilfe der MMP-Methode"*, Diss. ETH Nr.7792, Zürich, 1985.

[4] P. Regli, *"Automatische Wahl der sphärischen Entwicklungsfunktionen für die 3D-MMP Methode"*, Diss. ETH Nr.9946, Zürich, 1992.

[5] R. E. Collin, *"Field Theory of Guided Waves"*, IEEE Press Inc., New York, 1991.

[6] C. Müller, *"Grundprobleme der mathematischen Theorie elektromagnetischer Schwingungen"*, Springer-Verlag, Berlin, 1957.

[7] J. D. Jackson, *"Classical Electrodynamics"*, John Wiley & Sons, Inc., New York, 1975.

[8] J. Fröhlich, G. Klaus, *"Scattering in cavities"*, Radio Science Meeting, Ann Arbor, MI, USA, 1993.

[9] J. Fröhlich, G. Klaus, *"Computersimulationen von Feldverteilungen in geschirmten Räumen"*, Kleinheubacher Tagung, U.R.S.I. Commitee of the Federal Rep. of Germany, 1993.